

Palladium Nanoparticles Entrapped in Heavily Fluorinated Compounds

Mar Tristany,[†] James Courmarcel,[†] Philippe Dieudonné,[‡] Marcial Moreno-Mañas,^{*,†}
Roser Pleixats,[†] Albert Rimola,[†] Mariona Sodupe,[†] and Silvia Villarroya[†]

Department of Chemistry, Universitat Autònoma de Barcelona, Cerdanyola, 08193 Barcelona, Spain, and
Laboratoire des Colloïdes, Verres et Nanomatériaux, UMR CNRS 5587, Université de Montpellier II,
France

Received August 31, 2005. Revised Manuscript Received December 2, 2005

Palladium nanoparticles formed by the reduction of palladium(II) chloride with methanol or 2-propanol are stabilized by entrapment in solid heavily fluorinated compounds, as suggested by powder X-ray diffraction. Some of the stabilizers are fluorohydrocarbons without a functional group. Calculations suggest that minor amounts of Pd(II) on the surface of the nanoparticles might be the origin of attractive interactions with the negative periphery of perfluorinated chains (C_nF_{2n+1}). The role of sodium acetate in the precipitation of nanoparticles is underlined.

Introduction

Transition-metal nanoparticles have recently attracted a great deal of attention; their preparation, structure determination, and applications are topics of current interest.^{1,2} Among other interesting properties, their high specific surface renders them attractive in catalysis.^{1f,i,o,p}

In general, metallic nanoparticles are defined as having a diameter between 1 and 100 nm. They are surrounded by a shell of adequate protecting agent that prevents agglomeration.^{1b} The protecting agents can be broadly divided into three categories: (i) those that provide electrostatic stabilization, such as cationic and anionic surfactants; (ii) those that provide steric stabilization, including compounds possessing

a functional group endowed with a high affinity for metals such as thiols, sulfides, amines, and phosphines; and (iii) those that simply entrap nanoparticles, such as polymers (e.g., poly(vinylpyrrolidone)), cyclodextrins, and dendrimers. In all cases, protecting agents ought to interact in an attractive manner with the surface of the metal.

A priori, heavily fluorinated compounds are not ideal constituents of protecting shields for nanoparticles, because perfluorinated chains have a well-deserved reputation for having very small attractive interactions toward other materials and among themselves.³ As examples, we can mention the phobic properties of poly(tetrafluoroethylene) (PTFE) and the boiling point of perfluoroheptane (82 °C) compared with that of the corresponding alkane, heptane (92 °C). However, sometimes heavily fluorinated compounds and materials can stabilize transition-metal nanoparticles.⁴ Thus, polymers such as Nafion and PTFE, as well as dendrimers fluorinated in the surface,⁵ have been reported as being stabilizing agents, probably by the inclusion of nanoparticulated metal into the interstices of the polymer⁴ or the nonfluorinated core of the dendrimer.⁵ Other heavily fluorinated stabilizing agents are considered to act by classical stabilizing mechanisms. Thus, thiols C_nF_{2n+1}-CH₂CH₂-SH (*n* = 6, 8)⁶ and anions C_nF_{2n+1}-COO⁻ (*n* = 11–17)⁷ owe their stabilizing ability to the SH group and to the carboxylate rather than to the R_f moiety.

* To whom correspondence should be addressed. Phone: 34-935811254. Fax: 34-935811265. E-mail: marcial.moreno@uab.es.

[†] Universitat Autònoma de Barcelona.

[‡] Université de Montpellier II.

- (1) (a) Lewis, L. N. *Chem. Rev.* **1993**, *93*, 2693–2730. (b) Bradley, J. S. *The Chemistry of Transition Metal Colloids. In Cluster and Colloids, From Theory to Applications*; Schmid, G., Ed.; VCH: Weinheim, Germany, 1994; pp 459–544. (c) *Metal Clusters in Chemistry*; Braunstein, P., Oro, L., Raithby, P. R., Eds.; Wiley-VCH: Weinheim, Germany, 1998. (d) *Nanoparticles and Nanostructured Films: Preparation, Characterization and Applications*; Fendler, J. H., Ed.; Wiley-VCH: Weinheim, Germany, 1998. (e) Klabunde, K. J.; Mohs, C. *Nanoparticles and Nanostructured Materials. In Chemistry of Advanced Materials: An Overview*; Interrante, L. V., Hampden-Smith, M. J., Eds.; Wiley-VCH: New York, 1998; Chapter 7, pp 271–327. (f) Aiken, J. D., III; Finke, R. G. *J. Mol. Catal., A* **1999**, *145*, 1–44. (g) Templeton, A. C.; Wuelfing, W. P.; Murray, R. W. *Acc. Chem. Res.* **2000**, *33*, 27–36. (h) Rao, C. N. R.; Kulkarni, G. U.; Thomas, P. J.; Edwards, P. P. *Chem. Soc. Rev.* **2000**, *29*, 27–35. (i) Horn, D.; Rieger, J. *Angew. Chem., Int. Ed.* **2001**, *40*, 4330–4361. (j) Reetz, M. T.; Winter, M.; Breinbauer, R.; Thurn-Albrecht, T.; Vogel, W. *Chem.—Eur. J.* **2001**, *7*, 1084–1094. (k) Caruso, F. *Adv. Mater.* **2001**, *13*, 11–22. (l) Bönemann, H.; Richards, R. M. *Eur. J. Inorg. Chem.* **2001**, 2455–2480. (m) Rao, C. N. R.; Kulkarni, G. U.; Thomas, P. J.; Edwards, P. P. *Chem.—Eur. J.* **2002**, *8*, 28–35. (n) *Metal Nanoparticles: Synthesis, Characterization, and Applications*; Feldheim, D. L., Foss, C. A., Jr., Eds.; Marcel Dekker: New York, 2002. (o) Roucoux, A.; Schulz, J.; Patin, H. *Chem. Rev.* **2002**, *102*, 3757–3778. (p) Moreno-Mañas, M.; Pleixats, R. *Acc. Chem. Res.* **2003**, *36*, 638–643. (q) For a comprehensive review on gold nanoparticles see: Daniel, M.-C.; Astruc, D. *Chem. Rev.* **2004**, *104*, 293–346.
- (2) For a didactic explanation on the structure and properties of nanoparticles see: Cox, J. *Chem. Br. Sept.* **2003**, 21.

(3) *Organofluorine Chemistry: Principles and Commercial Applications*; Banks, R. E., Smart, B. E., Tatlow, J. C., Eds.; Plenum Press: New York, 1994.

(4) For a review see: Moreno-Mañas, M.; Pleixats, R. *Fluorous Nanoparticles. In Handbook of Fluorous Chemistry*; Gladysz, J. A., Curran, D. P., Horváth, I. T., Ed.; Wiley-VCH: Weinheim, Germany, 2004; Chapter 12.2, pp 491–507.

(5) (a) Crooks, R. M.; Zhao, M.; Sun, L.; Chechik, V.; Yeung, L. K. *Acc. Chem. Res.* **2001**, *34*, 181–190. (b) Crooks, R. M.; Lemon, B. I., III; Sun, L.; Yeung, L. K.; Zhao, M. *Top. Curr. Chem.* **2001**, *212*, 81–135.

(6) (a) Shah, P. S.; Holmes, J. D.; Doty, R. C.; Johnston, K. P.; Korgel, B. A. *J. Am. Chem. Soc.* **2000**, *122*, 4245–4246. (b) Yonezawa, T.; Onoue, S.; Kimizuka, N. *Adv. Mater.* **2001**, *13*, 140–142. (c) Yonezawa, T.; Onoue, S.; Kimizuka, N. *Langmuir* **2001**, *17*, 2291–2293.

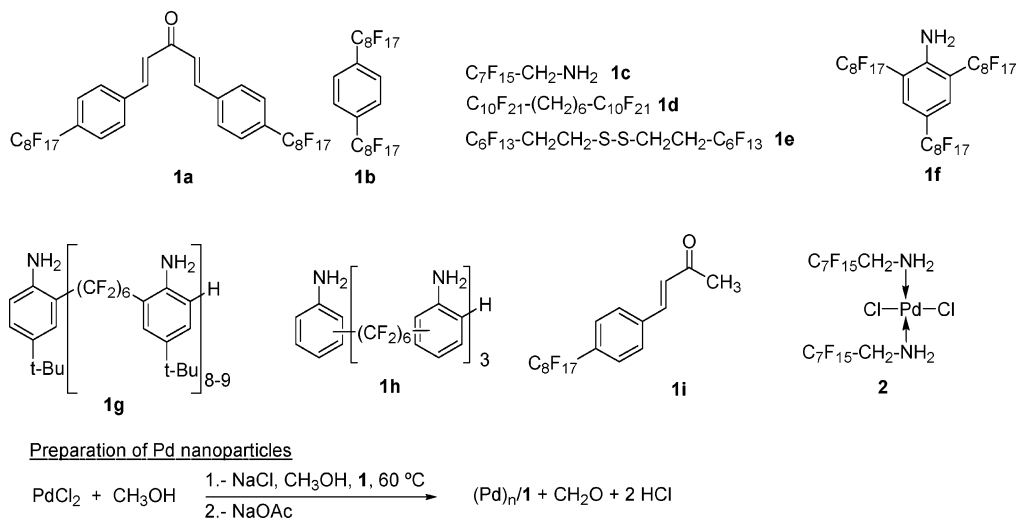


Figure 1. Heavily fluorinated compounds used in this study and the preparation of palladium(0) nanoparticles.

On the other hand, nanoparticles in the water core of a water-in-CO₂ emulsion have been stabilized by perfluorinated surfactants; however, stabilization seems to be caused by the hydrophilic polar part, whereas the perfluorinated moiety imparts solubility in CO₂.⁸

A different case reported by Klabunde refers to gold nanoparticles in the diameter range 3.4–5.0 nm that are formed by metal atom vapor deposition and stabilized by N(C₄F₉)₃.⁹ The mechanism by which the nonbasic tris-perfluorobutylamine could stabilize nanoparticles is unknown. Moreover, when this work was in progress, the stabilization of several metal-oxide nanoparticles (ZnO, ZrO₂, HfO₂, Al₂O₃, TiO₂, SnO₂, and WO_x) was achieved by molecularly well-defined perfluorinated compounds. Among them, the stabilizations of *n*-C₁₂F₂₆ and *n*-C₂₀F₄₂ are the most surprising, because no functional group is present.¹⁰ These nanoparticles were generated by the Karlsruhe microwave plasma process.¹⁰

We present here our preparation of palladium(0) nanoparticles stabilized by several molecularly well-defined heavily fluorinated compounds. As the family of fluorinated compounds is emerging as a serious possibility for stabilizing nanoparticles, we try to cast some light on the stabilization mechanism. Preliminary results were presented elsewhere.¹¹

Results and Discussion

Some time ago, we tried to prepare a fluorinated version of the palladium complex Pd(dba)₂ (dba = dibenzylidene-

acetone). This complex has been extensively used as a precatalyst in palladium-catalyzed reactions, and we thought the fluorinated version could be useful in organic–fluorous biphasic catalysis.¹² This project required 1,5-bis-(perfluorooctyl)-1,4-pentadien-3-one, **1a** (4,4′-bis-(perfluorooctyl)dibenzylideneacetone, Figure 1). When a well-known method for preparing Pd(dba)₂ was used with **1a**, we instead obtained palladium nanoparticles in which ketone **1a** defined the protecting shield (Table 1, entries 1–4).¹¹ This particular material was a recoverable catalyst under organic–fluorous biphasic conditions in some Suzuki-type cross-couplings and in Mizoroki–Heck reactions.^{11a}

An extension of these preliminary results has been undertaken. Thus, we present here our results with **1a** and with other simple and more easily accessible fluorinated compounds **1b–i** (Figure 1) as stabilizers as well as a possible explanation for the stabilizing ability of compounds featuring long perfluorinated chains.

Palladium nanoparticles were prepared by the reduction of palladium(II) chloride with methanol at 60 °C in the presence of sodium chloride and compound **1** (Figure 1). Sodium chloride forms ionic Na₂(Pd₂Cl₆), which is more soluble than PdCl₂. The further addition of sodium acetate induced precipitation of the material.

We established a protocol to make sure that palladium(0) nanoparticles were indeed formed instead of materials with other structures and compositions, as well as to ascertain if compounds **1** were the only substances present in the protecting shields. Finally, we deemed it important to check if compounds **1** had suffered any significant modification when surrounding the palladium nanoparticle. This protocol includes the following steps for each material: (i) determination of the decomposition point in °C; (ii) recording of the IR spectrum; (iii) recording of the NMR spectra; (iv) determination of the elemental analysis for all possible elements; and (v) checking if the sum of all percentages of

- (7) Lee, S. J.; Han, S. W.; Kim, K. *Chem. Commun.* **2002**, 442–443.
 (8) (a) Ji, M.; Chen, X.; Wai, C. M.; Fulton, J. L. *J. Am. Chem. Soc.* **1999**, *121*, 2631–2632. (b) Ohde, H.; Hunt, F.; Wai, C. M. *Chem. Mater.* **2001**, *13*, 4130–4135. (c) Ohde, H.; Wai, C. M.; Kim, H.; Kim, J.; Ohde, M. *J. Am. Chem. Soc.* **2002**, *124*, 4540–4541.
 (9) (a) Zuckerman, E. B.; Klabunde, K. J.; Olivier, B. J.; Sorensen, C. M. *Chem. Mater.* **1989**, *1*, 12–14. (b) Klabunde, K. J.; Youngers, G.; Zuckerman, E. J.; Tan, B. J.; Antrim, S.; Sherwood, P. M. *Eur. J. Solid State Inorg. Chem.* **1992**, *29*, 227–260.
 (10) (a) Lamparth, I.; Szabó, D. V.; Vollath, D. *Macromol. Symp.* **2002**, *181*, 107–112. (b) Szabó, D. V.; Lamparth, I.; Vollath, D. *Macromol. Symp.* **2002**, *181*, 393–398. (c) Vollath, D.; Lamparth, I.; Szabó, D. V. *Mater. Res. Soc. Symp. Proc.* **2002**, *703*, 303–308.
 (11) (a) Moreno-Mañas, M.; Pleixats, R.; Villarroja, S. *Organometallics* **2001**, *20*, 4524–4528. (b) Moreno-Mañas, M.; Pleixats, R.; Villarroja, S. *Chem. Commun.* **2002**, 60–61. (c) Moreno-Mañas, M.; Pleixats, R.; Tristany, M. *J. Fluorine Chem.* **2005**, *126*, 1435–1438.

- (12) (a) Horváth, I. T. *Acc. Chem. Res.* **1998**, *31*, 641–650. (b) Gladysz, J. A.; Corrêa da Costa, R. Strategies for the Recovery of Fluorous Catalysts and Reagents: Design and Evaluation. In *Handbook of Fluorous Chemistry*; Gladysz, J. A., Curran, D. P., Horváth, I. T., Ed.; Wiley-VCH: Weinheim, Germany, 2004; Chapter 4, pp 24–40.

Table 1. Palladium Nanoparticles Stabilized by Fluorous Compounds 1

entry	compd	initial molar ratio Pd:1 ^a	molar composition, wt % Pd ^b	yield (%) ^c	Ø (nm)	no. of atoms per particle ^d	X-ray	decomposition point (°C)
1	1a	0.55	Pd: 1a 1.15, 9.9%	78	3.6 ± 0.6	1.7 × 10 ³	<i>e</i>	140–145
2	1a	0.54	Pd: 1a 0.65, 6.0%	79	<i>e</i>	<i>e</i>	<i>e</i>	158–163
3	1a	4.64	Pd: 1a 4.08, 30.1%	100	5.1 ± 0.7	4.7 × 10 ³	<i>e</i>	170
4	1a	4.64	Pd: 1a 6.85, 37.6%	100	4.5 ± 0.9	3.2 × 10 ³	<i>e</i>	166–172
5	1b	1.55	Pd: 1b 1.71, 16.5%	93	16.0 ± 5.3	1.4 × 10 ⁵	fcc Pd	102–103
6	1b	0.50	Pd: 1b 0.54, 5.9%	96	13.0 ± 3.0	7.7 × 10 ⁴	fcc Pd	102–103
7 ^f	1b	1.54	Pd: 1b 1.06, 12.4%	59	4.4 ± 1.0	3.0 × 10 ³	fcc Pd	104–105
8	1b	1.53	Pd: 1b 1.09, 14.2%	78	25 ± 7	5.5 × 10 ⁵	fcc Pd	104–105
9	1c	0.50	Pd: 1c 3.86, 46.5%	79	4.0 ± 1.5	2.2 × 10 ³	<i>e</i>	240–245
10 ^f	1d	1.54	Pd: 1d 1.10, 10.3%	68	5 ± 2.0	4.4 × 10 ³	fcc Pd	115–116
11	1d	1.53	Pd: 1d 1.07, 10.0%	67	33 ± 9	1.3 × 10 ⁶	fcc Pd	112–115
12	1d	1.03	Pd: 1d 0.35, 3.1%	12	9.0 ± 2.8	2.6 × 10 ⁴	not clear	113–115
13	1e	2.26	Pd: 1e 2.85, 27.5%	43	<i>g</i>	<i>g</i>	not clear	155
14	1f	1.15	Pd: 1f 0.84, 6.3%	42	6.6 ± 0.7	9.9 × 10 ³	not clear	74–75
15 ^f	1f	1.54	Pd: 1f 1.31, 9.7%	74	12 ± 5	6.1 × 10 ⁴	fcc Pd	72–74
16	1f	1.54	Pd: 1f 1.06, 8.3%	65	26 ± 7	6.2 × 10 ⁵	fcc Pd	74–76
17	1g	8.38 (<i>n</i> = 9)	Pd: 1g 11.8, 23.6%	75	4.7 ± 0.6	3.8 × 10 ³	not clear	100–105
18	1h	2.05	Pd: 1h 9.32, 9.2%	<i>e</i>	11 ± 2	4.5 × 10 ⁴	<i>e</i>	<i>e</i>
19	1i	0.85	Pd: 1i 5.17, 56%	90	3.8 ± 0.8	1.9 × 10 ³	fcc Pd	90
20	1i	0.50	Pd: 1i 1.95, 27.4%	57	4.9 ± 0.9	4.1 × 10 ³	fcc Pd	84
21	1i	2.00	Pd: 1i 0.67, 11.1%	7	5.6 ± 1.1	6.3 × 10 ³	fcc Pd	80
22a ^h	1i	1.00	<i>g</i>	<i>g</i>	3.2 ± 0.6	1.2 × 10 ³	fcc Pd/ <i>i</i>	
22b ⁱ	1i	1.00	<i>g</i>	<i>g</i>	4.4 ± 1.2	3.0 × 10 ³	fcc Pd/ <i>j</i>	

^a In the form of PdCl₂. ^b Pd % determined by inductively coupled plasma (ICP). ^c Yield with respect to palladium. ^d From $0.74V_{\text{nanoparticle}}/V_{\text{atom}}$; 0.74 is the occupation factor for a face-centered cube crystal structure. ^e Not determined. ^f Reduction performed with 2-propanol. ^g See text. ^h Nanoparticles in solution before adding sodium acetate. ⁱ Nanoparticles precipitated after the addition of sodium acetate. ^j Determined by electron diffraction.

elemental analyses was near 100%; (vi) transmission electron microscopy (TEM) analyses to determine the size of the particles. (vii) More recently, we measured the powder X-ray diffraction (XRD) to have further evidence for the zero oxidation state of the metal and to gain information on the situation of the protecting **1**.

Data from steps i, ii, and iii were compared with those from compounds **1**. In steps iv and v, fluorine and oxygen percentages were calculated from the measured carbon percentages if spectroscopic data indicated that only **1** was present in the protecting shield. Because PdCl₂ was the source of metal, analytical values for chlorine below the limit of tolerance were sometimes determined.

The results are summarized in Table 1. First, we explored **1a** as a stabilizing agent. We studied the influence of the initial molar ratio PdCl₂:**1a** (entries 1–4). As expected, when working with a defect of palladium salt (ratio 0.54), nanoparticles possessing a smaller amount of metal (6–10%) were obtained (entries 1 and 2). However, the introduction of an excess of PdCl₂ (ratio 4.64) permitted the isolation of nanoparticles heavily loaded with metal (30–38%) (entries 3 and 4). However, this did not affect the size of the nanoparticles, which ranged between 4 and 5 nm in diameter. In all cases, IR, ¹H NMR, and ¹³C NMR spectra did not show differences from those of **1a**, although it could be argued that NMR corresponds to free stabilizing molecules in solution. The decomposition points were always higher than the melting point (mp) of **1a** (112–115 °C). The sum of elemental analyses was around 100% in all cases, and chlorine content was below the tolerance limit (±0.4). Narrow distributions of sizes were determined by TEM.

The preparation of **1a** was not easily reproducible. Therefore, we moved to simpler and more accessible compounds. First, we speculated with the angle between both C(aromatic)–CF₂ bonds in **1a**, 120° for any extended

conformation-maximizing conjugation. Therefore, we checked *m*-bis-(perfluorooctyl)benzene as well as its ortho isomer, which were devoid of stabilizing ability. However, the para isomer, **1b**,¹³ behaved very well. Ratios of PdCl₂:**1b** in the range 0.50–1.55 were studied (entries 5–8), and we observed an increase in the size of the nanoparticles when the PdCl₂:**1b** ratio was increased (entries 5, 6, and 8). The use of 2-propanol instead of methanol as the solvent and reducing agent gave much smaller nanoparticles (entry 7). Unfortunately, a lack of solubility in some reagents prevented the general use of 2-propanol. The decomposition point for all nanoparticles based on **1b** was very close to the mp of the stabilizer (mp 102–103 °C). Again, spectroscopic data permitted us to conclude that only **1b** was present in the stabilizing shield, despite some deviations from 100% in the sums of the elemental analyses for entries 7 and 8.

The commercially available 1*H*,1*H*-pentadecafluorooctylamine, **1c**, behaved differently. Thus, when liquid **1c** was added to the palladium(II) solution, a yellow precipitate of dichlorobis-(1*H*,1*H*-pentadecafluorooctylamino)palladium(II), presumably *trans*-**2** (mp 243 °C), was initially formed. Treatment of **2** with methanol in the usual way at 60 °C finally produced the nanoparticles (entry 9). Isolation of the amine group from the electron-attracting C₇F₁₅ chain by a simple methylene group still preserves part of the coordinating ability of the amine lone pair toward palladium(II), as evidenced by the formation of **2**. Therefore, in this case, the amino function of **1c** rather than that of the R_f moiety is most likely responsible for the stabilization, and **1c** was not further studied.

The stabilizing ability of the triblock polyfluorohydrocarbon 1,1,1,2,2,3,3,4,4,5,5,6,6,7,7,8,8,9,9,10,10,17,17,18,18,

Table 2. Palladium Nanoparticles Stabilized by Fluorous Compound **1b** and the Effect of the Experimental Conditions

entry	initial molar ratios (Pd: 1b :NaCl:NaOAc)	conditions ^a	molar composition, wt % Pd ^b	yield (%) ^c	Ø (nm)	no. of atoms per particle	X-ray or ED
1	1.0:0.65:1.0:7.5	24 h at 60 °C	Pd: 1b 1.09, 14.2%	78	25 ± 7	5.5 × 10 ⁵	fcc Pd ^{d,e}
2	1.0:0.65:1.0:12.1	24 h at 60 °C	Pd: 1b 1.71, 16.5%	93	16 ± 5	1.4 × 10 ⁵	fcc Pd ^{d,f}
3	1.0:1.0:2.2:2.0	24 h at 60 °C	no nanoparticles	0			
4	1.0:0.65:1.5:6.9	24 h at 60 °C	Pd: 1b 0.95, 10.3%	51	12 ± 2	5.8 × 10 ⁴	fcc Pd ^g
5	1.0:0.65:1.0:17.7	24 h at 60 °C	Pd: 1b 1.34, 13.2%	66	12 ± 2	5.9 × 10 ⁴	fcc Pd ^g
6	1.0:0.65:1.0:6.9	15 min at 60 °C	Pd: 1b 1.96, 19%	93	16 ± 2	1.5 × 10 ⁵	fcc Pd ^g
7	1.0:0.65:1.0:6.9	3 h at 60 °C	Pd: 1b 1.68, 15.9%	89	11 ± 4	4.8 × 10 ⁴	fcc Pd ^g

^a Conditions before the addition of NaOAc. ^b Pd % determined by ICP. ^c Yield with respect to palladium. ^d Determined by X-ray diffraction. ^e See Table 1, entry 8. ^f See Table 1, entry 5. ^g Determined by electron diffraction.

19,19,20,20,21,21,22,22,23,23,24,24,25,25,26,26,26-dotetracontafluorohexacosane or 11*H*,11*H*,12*H*,12*H*,13*H*,13*H*,14*H*,14*H*,15*H*,15*H*,16*H*,16*H*-perfluorohexacosane, **1d**,¹⁴ is striking because no functional group is present, and we can hypothesize that the stabilizing properties are due to the perfluorinated chains. Three batches of palladium nanoparticles stabilized by **1d** were prepared (entries 10–12). As for **1b**, a lower PdCl₂:**1d** ratio (1.03) gave smaller nanoparticles 9 nm in diameter (entry 12), whereas a higher ratio (1.54) gave a much bigger nanomaterial 33 nm in diameter (entry 11). The decomposition point was in all cases close to the mp of **1d** (104–105 °C). Similar to the case of **1b**, the use of 2-propanol afforded the smallest nanoparticles (entry 10).

Material stabilized with disulfide **1e** afforded a TEM that was difficult to interpret, indicating that the material probably presents a more complex organization (entry 13).

Next, we tested 2,4,6-tris-(perfluorooctyl)aniline, **1f**.¹⁵ This aniline is neither basic nor nucleophilic because of the accumulated electronic effect of three electron-withdrawing substituents and the steric effect produced by two perfluorinated chains in ortho positions. Therefore, it is reasonable to admit that the stabilizing effect is due to the perfluorinated chains (entries 14–16). Aniline **1f** also produced a good stabilization, the size depending again on the PdCl₂:**1f** ratio. Once more, smaller nanoparticles 6.5 nm in diameter were formed under a low ratio of 1.15 (entry 14), whereas a ratio as high as 1.54 produced a dramatic increase in size up to 26 nm (entry 16). It was possible to make nanoparticles in 2-propanol (entry 15) that were smaller than those made in methanol for the same PdCl₂:**1d** ratio (1.54). The decomposition points were close to the mp of **1f** (74–75 °C).

Polymers are typical stabilizing agents, and we mentioned the properties of PTFE and Nafion before. Therefore, we tested the short polymers **1g**¹⁵ and **1h**. Compound **1g** showed an excellent behavior (entry 17), and **1h** gave a material that exhibited excellent TEM images (entry 18). However, for unknown reasons, the sum of the elemental analysis gave a very low value, probably because of an analytical problem. Because of the limited amount of **1h** available, we did not further investigate this matter.

One question was opened when working with **1a**: is the coordination ability toward atomic palladium a prerequisite for the formation of nanoparticles? In our experience, this

condition helps but is not a prerequisite. Preparation and testing of ketone **1i** had a double purpose: the first was to contribute to an answer for the above question, and the second was to find good stabilizing agents that were simpler and more easily prepared than our initial **1a**.¹⁶ Indeed, **1i** does not coordinate atomic palladium but is an excellent stabilizer (entries 19–21). Surprisingly, by working within a very broad range of PdCl₂:**1i** ratios, we observed no dependence of size on the ratio. The mp of **1i** (90 °C) is once more close to the decomposition point of the nanoparticulated materials.

Furthermore, we created some experiments to ascertain the influence of other factors, such as the ratios of sodium chloride and acetate with respect to palladium, as well as the heating time elapsed before sodium acetate was added to the mixture (Table 2). The most salient feature is that the amount of sodium acetate is critical for the formation of nanoparticles (entry 3) that are not formed below a certain threshold. Also important is the observation that the required time elapsed before adding sodium acetate is very short (entry 6). Although some variations in size are observed in the results of Table 2, only these two clear conclusions can be drawn.

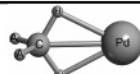

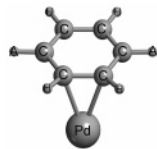
Next, we addressed the question of whether nanoparticles were present in solution before the addition of sodium acetate. We performed a standard preparation of nanoparticles stabilized by ketone **1i** (entry 22, Table 1). We examined the methanol solution before the addition of sodium acetate (entry 22a). Indeed, small nanoparticles of face-centered cubic Pd (fcc Pd) were detected by electron diffraction when some drops of the methanolic solution were deposited on the microscope grid and were left to evaporate. The residue contained small (fcc Pd) nanoparticles of 3.2 nm average diameter. The residue also contained larger aggregates, as is normal for a material that has not been submitted to any purification procedure. After this examination, we carried out the standard precipitation procedure by the addition of sodium acetate (entry 22b). In this case, nanoparticles were agglomerated; however, by examining the peripheral part of the agglomerations, we observed well-defined nanoparticles of 4.4 nm diameter. In summary, sodium acetate assists in the precipitation of the nanoparticles, probably by modifying

(14) Twieg, R. J.; Rabolt, J. F. *Macromolecules* **1988**, *21*, 1806–1811.

(15) Moreno-Mañas, M.; Pleixats, R.; Villarroja, S. *Synlett* **1999**, 1996–1998.

(16) The lettering of compounds **1** could look erratic. However, the large number of different materials prepared, featuring different metals and stabilizers, makes it advisable to avoid confusion by lettering compounds **1** in the same order in which they were prepared and tested and adhering to this lettering both in internal documents and externally in papers.

Table 3. Interaction Energies (kcal/mol), Pd–C Bond Lengths (Å), and Pd Net Atomic Charge for Pd–L Systems at the B3LYP Level of Theory

group	A	E_{int}	Pd–C	q_{Pd}	figure
alkanes	H	-7.2	2.502	0.03	
	CF ₃	-5.8	2.541	0.06	
alkenes	H	-32.3	2.138	0.16	
	CF ₃	-33.2	2.114	0.29	
aromatics	H	-21.3	2.222	0.17	
	CF ₃	-22.5	2.200	0.26	

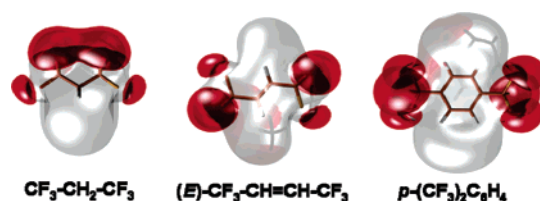
the ionic strength of the solution, but is not necessary for their formation.

We have commented on the lack of stabilizing properties of *o*- and *m*-bis-(perfluorooctyl)benzene. Moreover, negative results were obtained with the following heavily fluorinated compounds: 1*H*,1*H*,2*H*-perfluoro-1-decene (C₈F₁₇–CH=CH₂), perfluorooctylbenzene (C₈F₁₇–C₆H₅), 4-perfluorooctylbenzaldehyde (C₈F₁₇–C₆H₄–CHO), heptadecafluorononanoic acid (C₈F₁₇–COOH) and its sodium salt, and potassium perfluorooctanesulfonate (C₈F₁₇–SO₃K). If unsuccessful results with ionic salts are probably due to solubility, the negative results with the five compounds listed first led us to the intuition that a high melting point could be a beneficial factor. Moreover, liquids are useless as stabilizers unless a strong stabilizing group is present, as in **1c**.

Decomposition points, IR, and NMR data permitted us to anticipate that compounds **1** were not very affected when surrounding palladium nanoparticles. These aspects were studied by powder X-ray diffraction (vide infra). At this point, the hypothesis emerged that compounds **1** operated by an entrapment mechanism. We then decided to study the situation of the fluorine shield in the nanoparticles.

First, we undertook calculations on very simplified models to obtain information on the nature of the attractive forces binding together the phobic fluorinated compounds and palladium surfaces.

With the aim of understanding the interaction mechanism between Pd nanoparticles and stabilizers **1**, we performed calculations for Pd interacting with alkanes (CH₄ and CF₃–CH₂CF₃), alkenes (CH₂=CH₂ and (*E*)-CF₃CH=CHCF₃), and aromatics (benzene and *p*-(CF₃)₂C₆H₄) at the B3LYP level of theory^{17–19} (Table 3). Optimized geometries show that Pd does not interact with the fluorine atoms in any of the obtained structures, with Pd···F distances ranging from 3.2 to 3.7 Å. Instead, calculations suggest that the interaction

**Figure 2.** Electrostatic potential maps. Negative values are drawn in red and indicate regions to which positive charges are attracted.

between Pd and these organic molecules takes place through the C–H bond in alkanes, or through the C=C bonds of alkenes and aromatics. The order of Pd–molecule interactions is alkenes > aromatics > alkanes. These values correlate very well with the Pd–C distances: the larger the distances, the smaller the interaction energies. It is important to note that there is a charge transfer from Pd to the organic molecule that increases when CF₃ groups are present because of their electron-withdrawing character. Thus, the Pd–L interaction is enhanced when the organic compound contains CF₃ groups. CF₃CH₂CF₃ is the only exception, probably because of steric repulsion between CF₃ and Pd. Although calculations exclude the possibility that the fluorinated groups of compounds **1** are involved in the interaction mechanism with Pd(0), it could be that a limited number of Pd(II) atoms on the surface attract CF₃–(CF₂)_{*n*} chains that have a negative periphery. In fact, the optimization of Pd(II) interacting with these organic molecules shows an important F···Pd interaction, the computed F···Pd distances now being 2.1–2.2 Å. This is not surprising according to the electrostatic potential map of fluorinated compounds (see Figure 2), which shows that regions around CF₃ groups are areas of high electron density with negative potentials predisposed to interact with positive charges. Whereas the formation of charged nanoparticles is uncertain, it could be that compounds **1** surround the Pd(II) precursors before reduction, and after reduction remain surrounding Pd(0).

A study of the solid nature of some stabilizers **1** as well as of some of the derived nanoparticles was also undertaken. Panels a–c of Figure 3 clearly show that the diffraction patterns of pure **1b**, **1d**, and **1f** compounds exhibit diffraction peaks indicating that these compounds have a long-range ordered structure. Figure 3 also shows that the same

(17) (a) Becke, A. D. *J. Chem. Phys.* **1993**, *98*, 5648–5652. (b) Lee, C.; Yang, W.; Parr, R. G. *Phys. Rev. B* **1988**, *37*, 785–789.

(18) For geometry optimizations, we have described Pd with the LANL2DZ pseudopotential¹⁹ and C, F, and H atoms with the 6-31++G(d, p) basis set. Interaction energies have been computed adding an *f* function to Pd and using the 6-311++G(2df,2pd) basis.

(19) Hay, P. J.; Wadt, W. R. *J. Chem. Phys.* **1985**, *82*, 299–310.

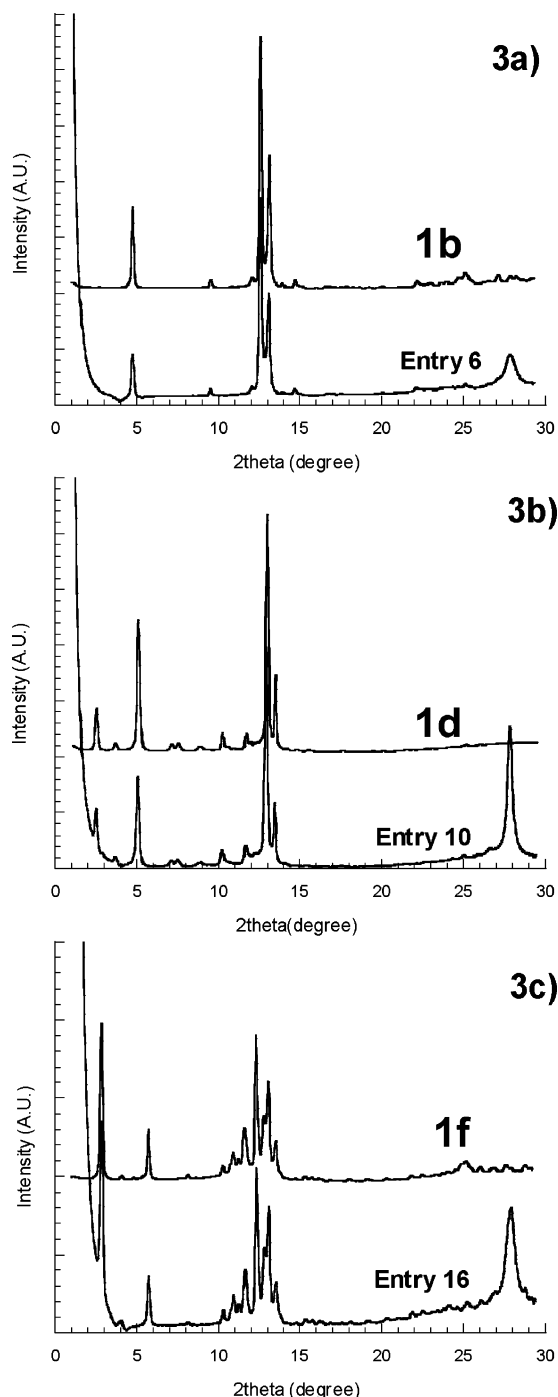


Figure 3. Powder X-ray diffraction patterns of (a) **1b**, (b) **1d**, and (c) **1f**, and of related nanoparticles.

crystalline phases of these fluorinated compounds exist in the related nanoparticle samples. The crystallization probably occurred after the nanoparticle synthesis procedure, when the synthesis medium was cooled to ambient temperature. The intensity peak observed in Figure 3 at around $2\theta = 28^\circ$ for all nanoparticle samples characterizes the existence of Pd(0). Moreover, for the same diffraction patterns, the observed increase in the scattering intensity at small 2θ values indicates the existence of heterogeneities on the 10 nm scale. For this sample series, we performed small-angle X-ray scattering experiments in the $0.08\text{--}1^\circ$ 2θ range in order to better characterize the nanoparticle form, size, and size polydispersity. We observed a power law increase in

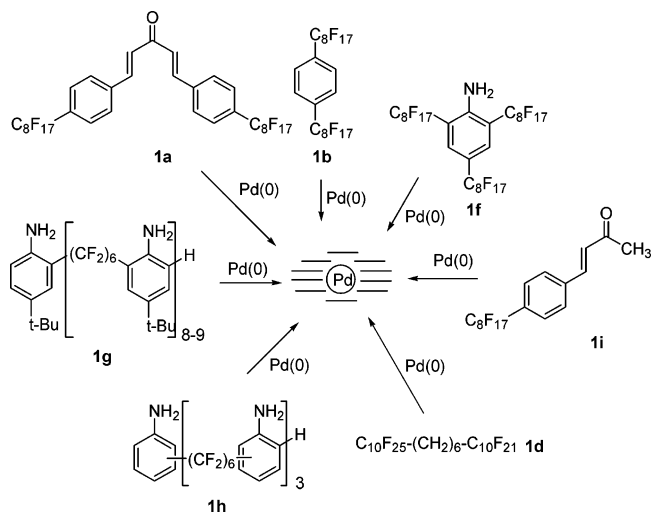


Figure 4. Entrapment of Pd(0) nanoparticles in the crystal structures of compounds **1**.

the intensity at small scattering angles in this entire 2θ range, meaning that a well-defined shape and size of the nanoparticles cannot be deduced from these measurements. These results are in accordance with TEM images showing nanoparticles connected with large necks and forming dense aggregates.

Conclusion

Palladium nanoparticles were prepared by the reduction of palladium(II) chloride with methanol or 2-propanol in the presence of stabilizing agents featuring long perfluorinated chains. Calculations and powder X-ray diffraction studies suggest that the nanoparticles are entrapped in the solid framework of the heavily fluorinated compounds (Figure 4).

Experimental Section

General Remarks. Compounds **1** were prepared as follows: **1a** as already described,^{11a} **1b** by the general and reliable method of McLoughlin and Thrower,¹³ **1c**, which is commercially available, **1d** by the method of Twieg and Rabolt,¹⁴ and **1f,g** as previously described by us.¹⁵ TEM and electron diffraction analyses were performed in the Servei de Microscòpia of the Universitat Autònoma de Barcelona, in a Hitachi H-7000 model at 100 kV or, for entries 4–7 of Table 2, in a JEOL JEM-2010 model at 200 kV. The material was suspended in an appropriate solvent, usually 1-bromoperfluorooctane or 1,1,2-trichloro-1,2,2-trifluoroethane. The suspension was sonicated for about 5 min, and one drop of the finely divided suspension was placed on a specially produced structureless carbon support film with a thickness of 4–6 nm; the samples were dried before observation.

Oligomer 1h. The general method for perfluoroalkylation of anilines was followed.¹⁵ To a stirred suspension of copper(I) oxide (3.87 g, 0.027 mol) in DMSO (5 mL) in inert atmosphere was added 1,6-diiodoperfluorohexane (3.00 g, 5.41 mmol). The mixture was heated at 130 °C for 20 min. A solution of aniline (0.50 g, 5.41 mmol) and DMSO (5 mL) was then slowly added, and the mixture was heated at 130 °C for 3 days under stirring and an inert atmosphere. The disappearance of aniline was monitored by GC. After cooling the solution to room temperature, we filtered off the solids, and the filtrate was partitioned between ethyl acetate and water. The organic phase was dried with anhydrous sodium sulfate. The solvent was evaporated, affording a brown residue that was

washed with aqueous sodium thiosulfate and then with active charcoal in boiling 1,2-dichloroethane. The charcoal was filtered off, and the dichloroethane was evaporated to give a gummy residue that was soluble in THF, ethyl acetate, chlorinated solvents, and perfluorinated solvents (Freon 113). IR (KBr): 3543, 3437, 1637, 1588, 1468, 1293, 1201, 1138 cm^{-1} . ^1H NMR (250 MHz, CDCl_3): δ 4.56 (broad s, NH_2), 4.9 (s, NH_2), 6.70 (m), 7.25 (m), 7.50 (m). FAB-MS: m/z 442, 784, 884, 1175, 1275, 1566, 1657, 1918, 2058; the superscript number 3 in formula **1h** is an average. Anal. Calcd for $\text{C}_{42}\text{H}_{22}\text{F}_{36}\text{N}_4$: C, 39.81; H, 1.74; N, 4.42. Found: C, 39.99; H, 1.74; N, 4.20.

4-(4-Perfluorooctyl)phenyl)-3-buten-2-one, 1i. This compound was prepared by the general method of Irie and Watanabe.²⁰ 4-(Perfluorooctyl)benzaldehyde²¹ (700 mg, 1.335 mmol), zinc diacetate dihydrate (586 mg, 2.670 mmol), and 2,2'-bipyridine (375 mg, 2.401 mmol) were dissolved in DMF (100 mL). Diazabicycloundecene (DBU) (0.305 mL, 2.04 mmol) and acetone (4.97 mL, 66.8 mmol) were added to the DMF solution, and the mixture was heated overnight at 120 °C. The crude was partitioned between 1 M HCl and ethyl acetate. The organic layer was washed with water, brine, and water and dried with sodium sulfate. The solvent was evaporated, and the residue was passed through a column of silica gel with 80:20 hexanes–ethyl acetate to afford **1i** as a white solid. Mp: 87 °C. IR (ATR): 1628, 1614, 1194, 1145, 1112 cm^{-1} . ^1H NMR (CDCl_3 , 250 MHz): δ 2.40 (s, 3H), 6.78 (d, $J = 16.3$ Hz, 1H), 7.52 (d, $J = 16.3$ Hz, 1H), 7.59–7.65 (m, 4H). ^{13}C NMR (CDCl_3 , 62.5 MHz): δ 27.8, 105.5–120.0, 127.5 (t, $J = 6.7$ Hz), 128.2, 129.3, 130.4 (t, $J = 24.8$ Hz), 138.2, 141.1, 197.8. MS (70 eV): m/z 566.1 (18, M + 1), 565.1 (100, M).

Typical Preparations of Nanoparticles. Table 1, Entry 5. A mixture of palladium chloride (0.180 g, 1.015 mmol), sodium chloride (0.058 g, 1.025 mmol), and methanol (10 mL) was stirred at room temperature for 24 h. The mixture was filtered through a glass wool plug. Additional methanol (10 mL) was added to the filtrate. The solution was heated at 60 °C under stirring; 1,4-bis-(perfluorooctyl)benzene, **1b** (0.600 g, 0.656 mmol), was added, and the mixture was heated (60 °C) under stirring for 24 h. Sodium acetate (1 g) was then added, and stirring was maintained at room temperature for 1 h. The formed black solid was filtered, washed successively with methanol, water, and acetone; it was then dried to afford 0.605 g of a black solid that was soluble in perfluorooctane, perfluorooctyl bromide, and 1,1,2-trichloro-1,2,2-trifluoroethane and

had a decomposition point at 102–103 °C. Extraction of the methanolic filtrate with perfluorooctane did not give additional material. The IR and ^1H NMR spectra of the solid were identical to those of **1b**. Elemental analysis: C, 23.93; H, 0.34; Cl, <1; Pd, 16.51. The size of the nanoparticles is 15–20 nm, as determined by transmission electron microscopy (TEM).

Table 1, Entry 8. A mixture of palladium chloride (179 mg, 1.010 mmol) and sodium chloride (59.1 mg, 1.01 mmol) in methanol (10 mL) was stirred for 24 h at room temperature. The solution was filtered through glass wool and diluted with additional methanol (10 mL). 1,4-Bis-(perfluorooctyl)benzene (602 mg, 0.658 mmol) was added, and the mixture was heated at 60 °C for 24 h. Sodium acetate trihydrate (1.03 g, 7.57 mmol) was then added, and the mixture was cooled while it was being stirred. The black precipitate was centrifuged and washed successively with methanol, water, and acetone to afford a gray-black solid (586 mg). Decomposition point: 104–105 °C. IR (ATR): 1416, 1370, 1300, 1193, 1144, 1112, 1095, 948, 852, 656 cm^{-1} . ^1H NMR (250 MHz, $\text{CFCl}_2\text{-CClF}_2 + \text{CDCl}_3$): δ 7.80 (s, 4H, arom). Elemental analysis found: C, 32.57 and 32.29; H, 0.25 and 0.29; Cl, <0.5%; Pd, 14.23; F, 79.36 (calculated from % C); sum: 126.3. TEM: 25 ± 7 nm ($\text{C}_8\text{F}_{17}\text{-Br}$, 108 particles).

X-ray Crystallographic Study. X-ray diffraction experiments were carried out on solid powders in 1 mm diameter glass capillaries at 22 °C in the LCVN laboratory, Montpellier, France. We worked in a transmission configuration. A copper rotating anode X-ray source (functioning at 4 kW) with a multilayer focusing Osmic monochromator giving high flux (108 photons/s) and punctual collimation was employed. An image plate 2D detector was used. X-ray diagrams were obtained that gave the diffracted intensity as a function of the diffraction angle 2θ . The scattering intensity was corrected by transmission and intensity background coming from scattering by an empty capillary.

Acknowledgment. Financial support from the Ministry of Science and Technology of Spain (Projects 2002BQU-04002 and CTQ2005-04968) and Generalitat de Catalunya (Projects 2001SGR00181 and 2005SGR00305) is gratefully acknowledged.

Supporting Information Available: TEM images and X-ray diffraction patterns of the nanoparticles for most of the entries in Tables 1 and 2 (pdf). This material is available free of charge via the Internet at <http://pubs.acs.org>.

CM051967A

(20) Irie, K.; Watanabe, K. I. *Bull. Chem. Soc. Jpn.* **1980**, *53*, 1366–1371.

(21) Pozzi, G.; Colombani, I.; Miglioli, M.; Montanari, F.; Quici, S. *Tetrahedron* **1997**, *53*, 6145–6162.